MILLIMETER ARRAY
MEMO NO. 81

Evaluating the MMA Compact Configuration Designs

M.A. Holdaway

March 28, 1992

1 Introduction

Since the MMA will spend a large fraction of its time observing objects larger than the its primary beam and mosaicing will be required, the MMA design must ensure that the ability to produce good mosaic images is not significantly compromised for any observable sources. In a mosaic observation, all spatial frequencies out to the maximum sampled by the array must be measured for reliable image reconstruction. In the homogeneous array design, the short spacings are measured in an indirect manner (Cornwell, Holdaway, and Uson, 1992). An interferometer of baseline B is sensitive to spatial frequencies between $B - D/\lambda$ and $B + D/\lambda$ (Ekers and Rots, 1981). It has been found that good images can be produced by mosaicing the data from a close-packed array and total power data from an antenna of the same size as the interferometric elements. In fact, in the MMA design, the interferometric elements will perform the total power measurement. The homogeneous array design requires that the antennas be very close together. If the antennas are too far apart (say 2D), then there will be no overlap between the interferometer and total power sensitivities at around D/λ, resulting in poor images. On the other hand, the antenna design and safety require that the antennas be somewhat farther apart than D.

When observing low declination sources at the VLA, the north arm is extended to the next larger array (D goes to DnC). The extended north arm mainly serves to produce a nearly circular beam for sources around $\delta = -25°$. While having a circular beam for low declination observations is also important for the MMA, there are additional constraints on the MMA compact configuration: the beam shape should not change too much as a source is tracked through a few hours for mosaic observations, the short spacing coverage must be very good, and there cannot be too much shadowing. To some extent, these requirements are incompatible, and some compromises must be made, especially for low declinations. For efficient observations of low declination sources, multiple compact configurations must be designed. Ge (1992) proposes a number of possible compact configurations for the MMA which cover observable declinations. Ge has concentrated on each configuration's beam shape and u,v coverage. Shadowing was a driving force in each array layout, but Ge's memo does not quantify shadowing. Through numerical simulations, I evaluate the success of these various configurations at producing good mosaic images and determine the loss of sensitivity due to shadowing over a range of declinations.

2 Simulations

Without noise or errors, mosaicing with a homogeneous array gives excellent images for a wide variety of configurations. For simulations of different array configurations to be meaningful, errors must be added to the simulated data. Considering the current MMA design specifications, the most damaging error for mosaicing is the antenna pointing. A pointing error model with both systematic and random terms resulting in $1''\!.2$ rms pointing has been used in these simulations (Holdaway, 1990). Mosaic images degrade smoothly with source strength when both pointing errors and Gaussian noise are added to the simulated data. Images of weak sources will be limited by thermal noise, and only images of very bright sources will be limited by pointing errors. Therefore, Gaussian noise has not been added.

An optical image of an HII region in M31 was used for the model brightness distribution (Braun, 1989). Sampling at $\lambda/2D$ with 8 m dishes at 230 GHz, 49 pointings were required to span this object. Total power was measured with the same 8 m dishes. Ge (1992) points out the severe ellipticity of the synthesized beam when low declination, high hour angle observations are made. In order to obtain a more uniform beam over all pointings in the mosaic observation, each pointing was observed twice, once at $-$HA and once at $+$HA. The simulated observations lasted 3 hours, ranging from -1.5 to 1.5 hours. This may not be representative of actual observations, which will be limited by increased atmospheric opacity at low elevations; sources around $\delta = 35°$ may be effectively observed for over six hours, while a source at $\delta = -25°$ might only be observed for two hours. However, the constant range in observed hour angle makes comparison of observations of sources at different declinations much easier.

Since the simulation and imaging process takes a good deal of computer time, simulations were made only for the range of declinations at which an array is likely to be useful, which is defined by shadowing and beamshape criteria. For the standard D array, simulations were generally performed with a declination increment of 20°, and for the low declination arrays, the declination increment is 10°.

The simulated data were reduced using the nonlinear *mosaic* algorithm (Cornwell, 1988; Cornwell, Holdaway, and Uson, 1992) carried out to 40 iterations. The resulting images are then evaluated in three ways: dynamic range, defined as the image peak divided by the off-source rms; the image fidelity, which is a measure of the on-source signal to noise ratio; and by the integrated error on spacings ranging from 0 to 12 meters. The fraction of shadowed antennas over a 3 hour observation is also used to evaluate the configurations.

3 Configurations

Each array configuration presented here consists of 40 antennas, 8 m in diameter, as specified in the MMA proposal. The standard D array (compact configuration) used in Ge's memo is satisfactory for observing over most of the sky. Ge introduces two series of arrays for observing southern sources. In the MIXED series (option 1, option 2, and option 3 in Ge's memo), the standard packed D array sits in the center of the elliptical C array. As lower declination sources are observed, some of the antennas begin to shadow each other. The series of MIXED arrays are

Table 1: Compact Configuration Nomenclature

Name in Ge (1992)	Name in this memo
D	D, standard array
option 1	MIXED-1
option 2	MIXED-2
option 3	MIXED-3
DEC-20-EL	OPTIMIZED−20
DEC-29	OPTIMIZED−29
DEC-30	OPTIMIZED−30
DEC-30.PRAC	OPTIMIZED−30P

formed by removing the shadowed antennas from the D array and placing them onto selected C array stations. The primary advantage to this scheme is that no extra stations need to be built for the low dec arrays. The second series of low dec arrays is formed by removing the shadowed antennas and placing them at new stations which are optimized for a particular declination. I will call these arrays the OPTIMIZED series, and Ge refers to these arrays as DEC-20-EL, DEC-29, DEC-30.PRAC, and DEC-30. A complete list of the names used in Ge and in this memo is presented in Table 1.

4 Results

The results of the simulations are summarized in Figures 2 through 4. Of these four measures of configuration or image quality, only the fraction of shadowed baselines possesses an absolute meaning (i.e., lower sensitivity). The primary use of these quality measures is to design array configurations that have uniform imaging properties over the range of observable declinations. Hence, the fidelity index, dynamic range, short baseline integrated error, and shadow fraction should be used as *relative* measures of each configuration's imaging quality.

4.1 Short Spacing Reconstruction Errors

There is A fundamental tradeoff in a homogeneous array between getting the antennas close enough together to maximize the short spacing coverage and getting the antennas a bit further apart to minimize shadowing. Short spacing reconstruction errors are largely caused by pointing errors and exacerbated by poor short spacing u,v coverage. The short spacing reconstruction errors can be quantified by integrating over the fractional error in the Fourier plane out to some maximum spacing, chosen here to be 12 m.

What level of short spacing error is acceptable? The standard D array has a fractional short spacing reconstruction error of about 0.02 over its useful range of declination. The MIXED-3 and OPTIMIZED−29 configurations are designed to observe the lowest declination sources with minimal shadowing, and the antennas are relatively far apart. It is not surprising that these two configurations produce images which exceed the short spacing error criterion as they are the only configurations which do not result in excessive shadowing at very low declinations. Poor coverage of the short spacings also leads to decreased dynamic range and fidelity index.

4.2 Shadowing

How much shadowing is acceptable? A similar question floating around is: "How far in hour angle should one observe, or how much increase in opacity is acceptable?". One guess is that the airmass averaged over the observation should be about 20% higher than the airmass at transit. We might as well be consistent in our guessing: shadowing will be assumed important when it exceeds 20%.

Under what conditions does shadowing exceed 20%? The standard D configuration becomes severely shadowed for $\delta > 75°$ and $\delta < -10°$. Most of the low declination configurations have shadowing trouble for $\delta < -20°$. The OPTIMIZED−29 configuration does not have shadowing trouble until $\delta = -40°$ and the OPTIMIZED−30 configuration hits 20% shadowing at about $\delta = -25°$. High shadowing in the D configuration at high dec can be solved by observing high dec sources near transit with any of the low dec arrays. The shadowing at low dec is a real problem with the configurations at hand. A source at $\delta = -40°$ will have about 50% shadowing. Reducing the length of the simulated observation from 3 to 1.5 hours does not improve the shadowing a great deal. If such high shadowing fractions at the lowest declinations is unacceptable, new low declination arrays need to be designed.

4.3 Dynamic range and Fidelity Index

What values of dynamic range and fidelity index are acceptable? The canonical values from mosaic simulations with a wide range of errors are DR∼1000:1 and FI∼20. The standard D configuration produces images which are of this quality or better over its useful range of declinations, though the dynamic range falls off around $\delta = -10$. For low declination arrays, image quality decreases with declination, and DR decreases to about 500:1 and FI remains around 20. The MIXED-3 and OPTIMIZED−29 configurations do not perform well. It is interesting that the best images result when the source is directly overhead. Of the low dec arrays which were tested at $\delta = 80°$, the OPTIMIZED−30 configuration produces images with the best dynamic range and fidelity.

4.4 Summary of Results

A number of conclusions can be drawn from the simulation results:

- The standard D array performs well for $-10° < \delta < 75°$.
- The OPTIMIZED configurations clearly outperform the MIXED configurations.
- A low declination array can be used to observe sources at $\delta > 75°$.

- For the arrays used to observe extremely low dec sources, there is a tradeoff between shadowing and short spacing coverage. The best overall low dec array (OPTIMIZED−30) will be 20% shadowed at $\delta = -25°$ and over 50% shadowed at $\delta = -40°$. Arrays with less shadowing can be designed, but close attention must be paid to the quality of their images.

-

- The low declination configurations suffer from some image degradation. The fidelity index is a reasonably high 20, but the dynamic range drops to about 500:1.

- The beam shape has not been considered in this analysis. Considering only the quality measures used in this document, reasonably good imaging over the observable sky can be achieved using the standard D array for $-10° < \delta < 75°$ and use the OPTIMIZED−30 array for $\delta < -10°$ and $\delta > 75°$.

5 References

Cornwell, T.J. 1988 A+A.

Cornwell, T.J., Holdaway, M.A., and Uson, J. 1992 In Preparation.

Ekers and Rots 1981

Ge, J.P. 1992 MMA Memo 80

Holddaway, 1990 MMA Memo 61

Braun, R. 1989 MMA Memo 54

Figure 1: Fractional error in the u,v plane integrated from 0 to 12 m. Top graph is for D and MIXED configurations, bottom graph is for D and OPTIMIZED configurations.

Figure 2: Fraction of shadowed baselines for a three hour mosaic for the different configurations and various declinations. Top graph is for D and MIXED configurations, bottom graph is for D and OPTIMIZED configurations.

Figure 3: Dynamic range for different configurations and declinations. Top graph is for D and MIXED configurations, bottom graph is for D and OPTIMIZED configurations.

Figure 4: Fidelity index for different configurations and declinations. Top graph is for D and MIXED configurations, bottom graph is for D and OPTIMIZED configurations.

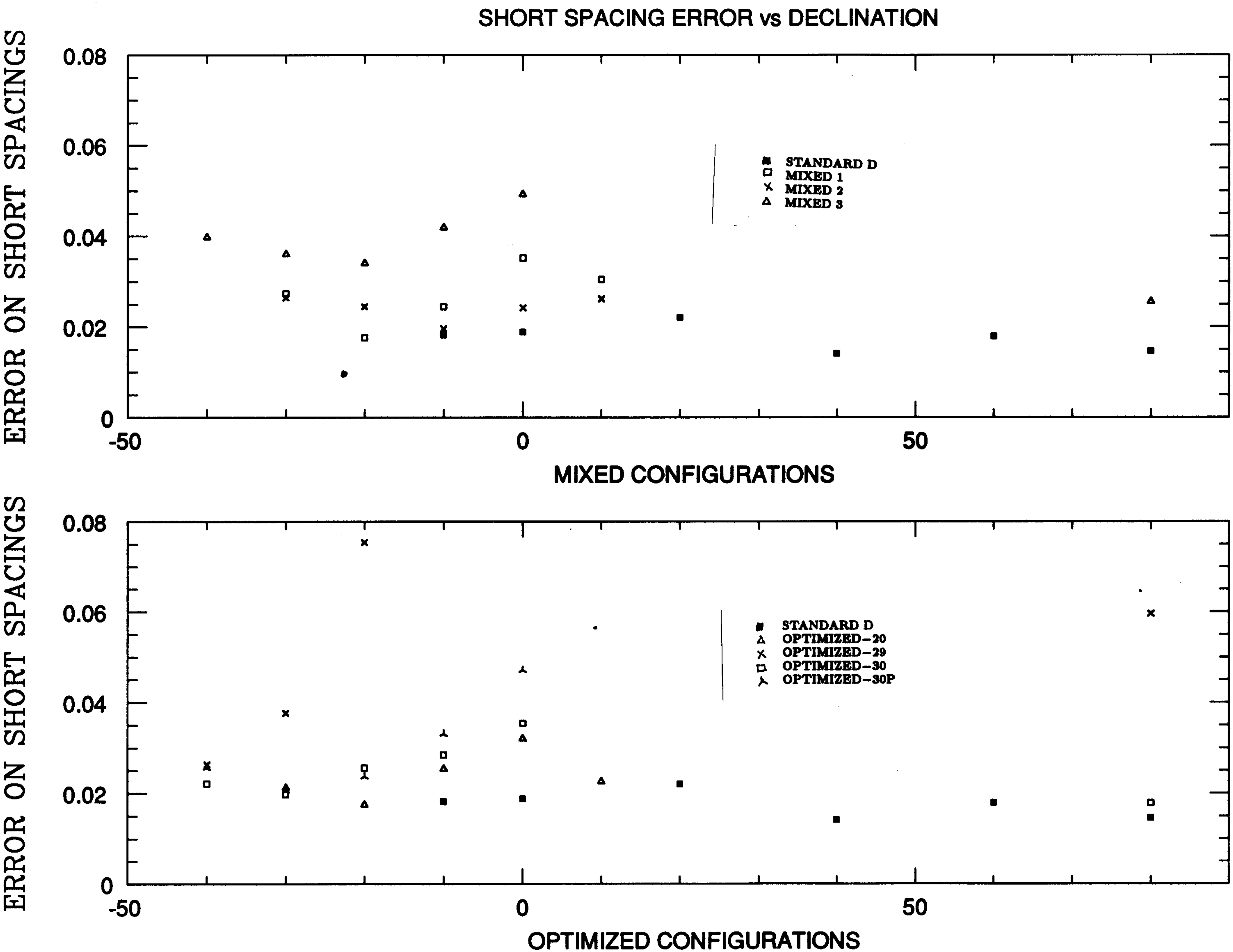

SHORT SPACING ERROR vs DECLINATION
ERROR ON SHORT SPACINGS
0.08
0.06
0.04
0.02
0
-50
0
50
MIXED CONFIGURATIONS
STANDARD D
MIXED 1
MIXED 2
MIXED 3
ERROR ON SHORT SPACINGS
OPTIMIZED CONFIGURATIONS
STANDARD D
OPTIMIZED-20
OPTIMIZED-29
OPTIMIZED-30
OPTIMIZED-30P

Figure 1

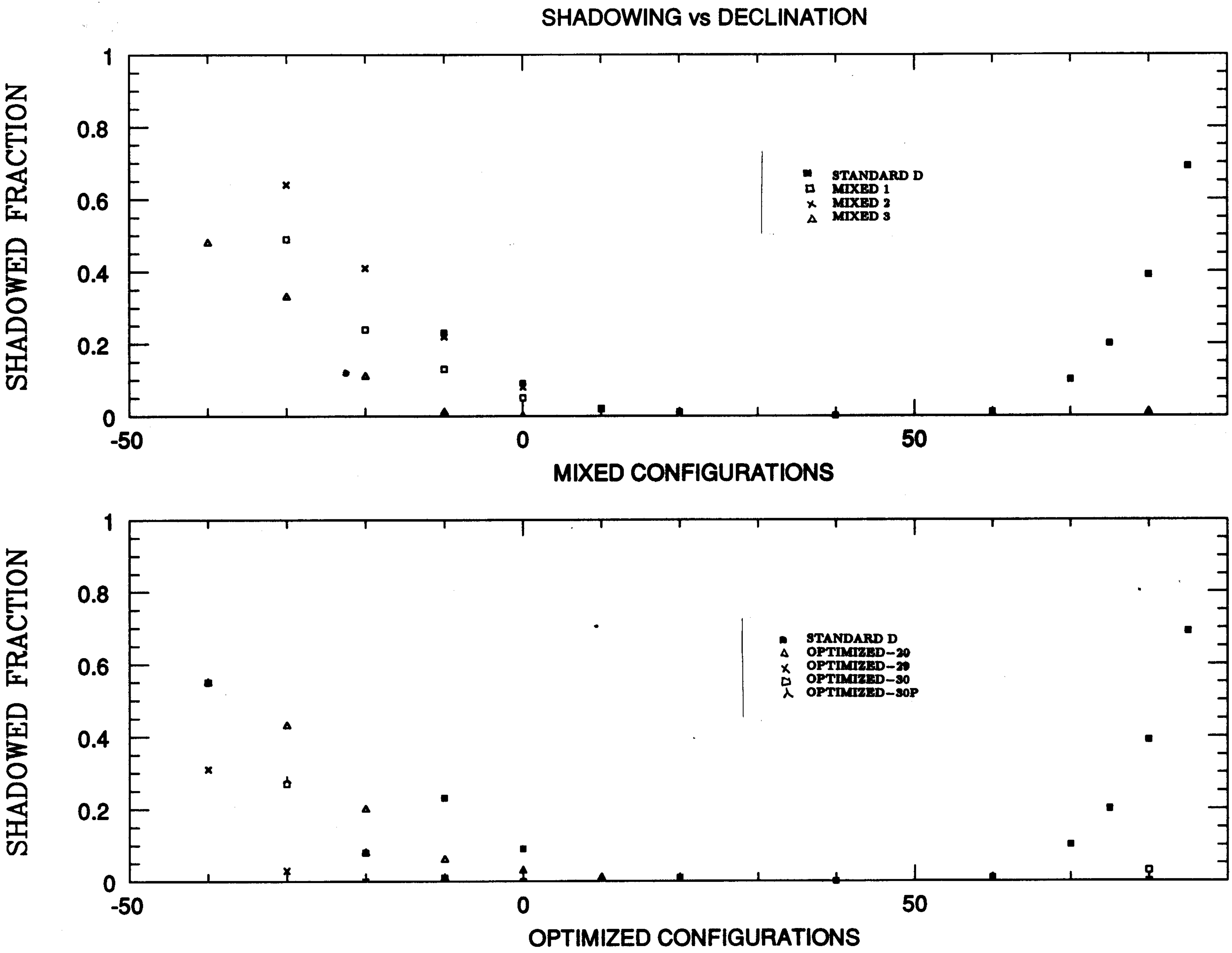
SHADOWING vs DECLINATION
SHADOWED FRACTION
0
0.2
0.4
0.6
0.8
1
-50
0
50
MIXED CONFIGURATIONS
STANDARD D
MIXED 1
MIXED 2
MIXED 3
SHADOWED FRACTION
0
0.2
0.4
0.6
0.8
1
-50
0
50
OPTIMIZED CONFIGURATIONS
STANDARD D
OPTIMIZED-20
OPTIMIZED-29
OPTIMIZED-30
OPTIMIZED-30P

Figure 2

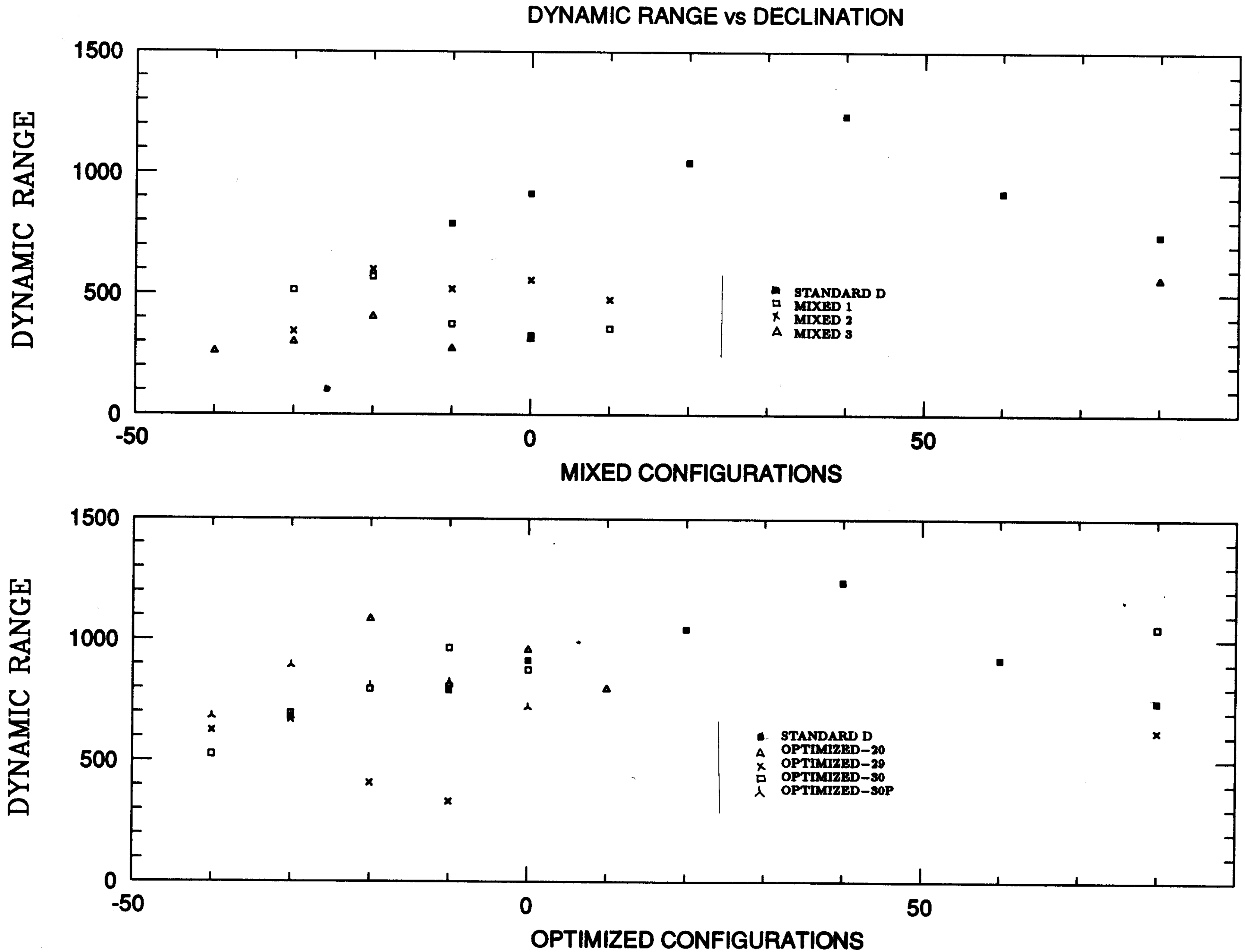
DYNAMIC RANGE vs DECLINATION
DYNAMIC RANGE
1500
1000
500
0
-50
0
50
MIXED CONFIGURATIONS
STANDARD D
MIXED 1
MIXED 2
MIXED 3
DYNAMIC RANGE
1500
1000
500
0
-50
0
50
OPTIMIZED CONFIGURATIONS
STANDARD D
OPTIMIZED-20
OPTIMIZED-29
OPTIMIZED-30
OPTIMIZED-30P

Figure 3

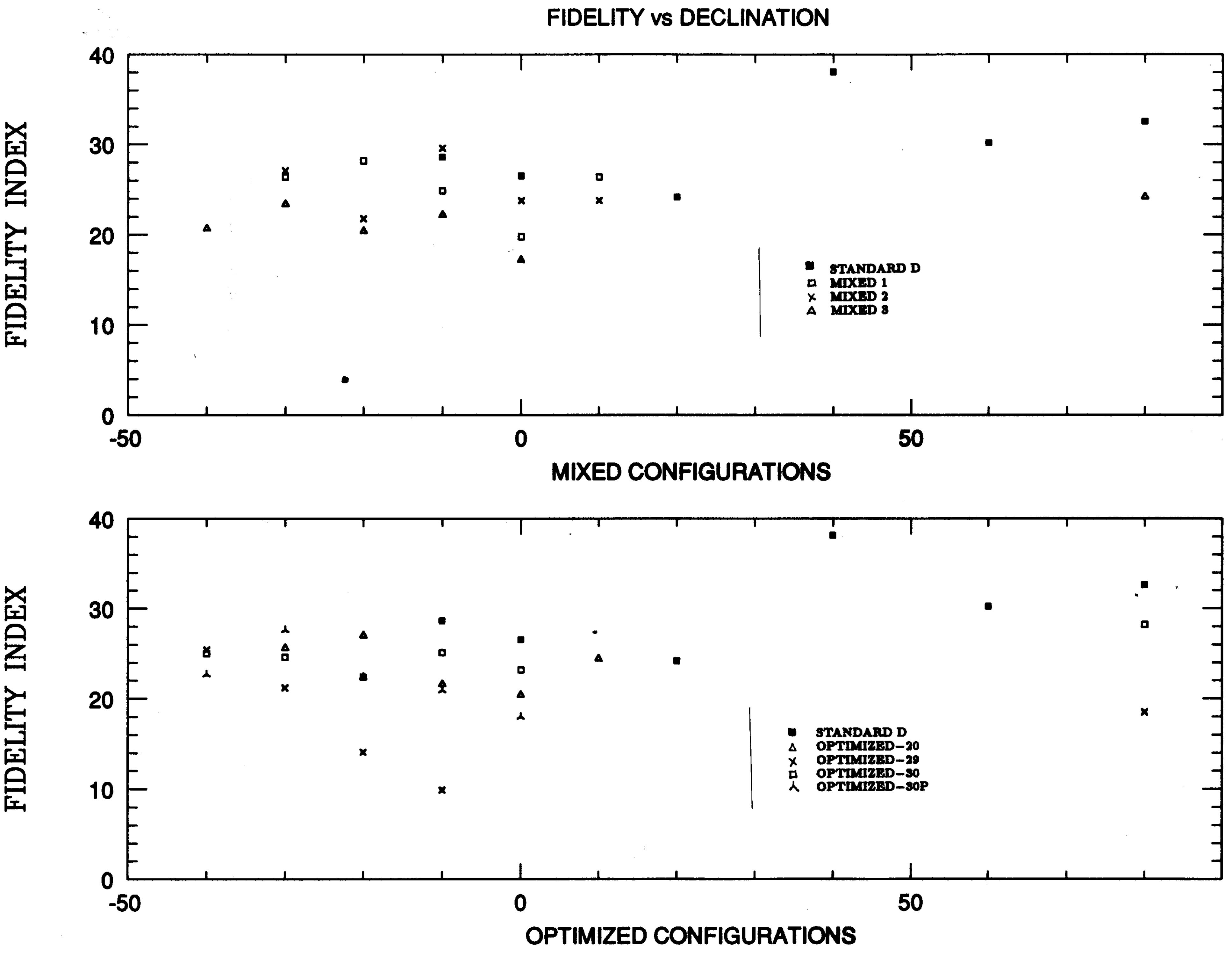
FIDELITY vs DECLINATION
FIDELITY INDEX
40
30
20
10
0
-50
0
50
MIXED CONFIGURATIONS
STANDARD D
MIXED 1
MIXED 2
MIXED 3
FIDELITY INDEX
OPTIMIZED CONFIGURATIONS
STANDARD D
OPTIMIZED-20
OPTIMIZED-29
OPTIMIZED-30
OPTIMIZED-30P

Figure 4